



Measuring Soil Water Content with Ground Penetrating Radar A Decade of Progress

Klotzsche, A.; Jonard, F.; Zibar, Majken Caroline Looms; van der Kruk, J.; Huisman, J. A.

Published in:
Vadose Zone Journal

DOI:
[10.2136/vzj2018.03.0052](https://doi.org/10.2136/vzj2018.03.0052)

Publication date:
2018

Document version
Publisher's PDF, also known as Version of record

Document license:
[CC BY-NC-ND](#)

Citation for published version (APA):
Klotzsche, A., Jonard, F., Zibar, M. C. L., van der Kruk, J., & Huisman, J. A. (2018). Measuring Soil Water Content with Ground Penetrating Radar: A Decade of Progress. *Vadose Zone Journal*, 17(1), [180052].
<https://doi.org/10.2136/vzj2018.03.0052>

Update

Core Ideas

- There has been tremendous progress in GPR as a tool for soil water content determination.
- Numerous studies have shown the potential of GPR to detect and map SWC.
- We highlight new possibilities and achievements for GPR acquisition and processing strategies.
- Quantitative SWC detection and hydrological parameter estimation are possible using GPR.
- We encourage other communities to embrace GPR as a tool for SWC determination.

A. Klotzsche, F. Jonard, J. van der Kruk, and J.A. Huisman, Institute of Bio- and Geosciences, Agrosphere (IBG-3), Forschungszentrum Jülich GmbH, Jülich, Germany; F. Jonard, Earth and Life Institute, Univ. catholique de Louvain, Louvain-la-neuve, Belgium; M.C. Looms, Dep. of Geosciences and Natural Resource Management, Univ. of Copenhagen, Copenhagen, Denmark. *Corresponding author (a.klotzsche@fz-juelich.de).

Received 20 Mar. 2018.
Accepted 20 Apr. 2018.

Citation: Klotzsche, A., F. Jonard, M.C. Looms, J. van der Kruk, and J.A. Huisman. 2018. Measuring soil water content with ground penetrating radar: A decade of progress. *Vadose Zone J.* 17:180052. doi:10.2136/vzj2018.03.0052

© Soil Science Society of America.
This is an open access article distributed under the CC BY-NC-ND license (<http://creativecommons.org/licenses/by-nc-nd/4.0/>).

Measuring Soil Water Content with Ground Penetrating Radar: A Decade of Progress

A. Klotzsche,* F. Jonard, M.C. Looms, J. van der Kruk, and J.A. Huisman

Tremendous progress has been made with respect to ground penetrating radar (GPR) equipment, data acquisition, and processing since the establishment of GPR as a tool for soil water content determination in vadose zone hydrology about 25 yr ago. In this update, we aim to provide a critical overview of recent advances in vadose zone applications of GPR with a particular focus on new possibilities for multi-offset and borehole GPR measurements, the development of quantitative off-ground GPR methods, full-waveform inversion of GPR measurements, the potential of time-lapse GPR measurements for process investigations and hydrological parameter estimation, and recent improvements in GPR instrumentation. We hope that this update encourages the soil hydrology, groundwater, and critical zone community to embrace GPR as a viable tool for soil water content determination and the elucidation of subsurface hydrological processes.

Abbreviations: CMP, common midpoint; EM, electromagnetic; ERT, electrical resistivity tomography; FWI, full-waveform inversion; GPR, ground penetrating radar; SWC, soil water content; VRP, vertical radar profiling; WARR, wide-angle reflection and refraction.

In many different disciplines ranging from hydrology and soil science to meteorology, knowledge about the spatiotemporal variability of soil water content (SWC) is important (Famiglietti et al., 2008). The SWC determines the separation of precipitation into surface runoff and infiltration, and thus affects erosion, river discharge, and groundwater recharge. At the field scale, SWC is a major control on plant growth and crop quality (Vereecken et al., 2016). It is clear that many applications crossing a range of scales would benefit from an improved understanding and description of the spatiotemporal variation of SWC, and the incorporation of such spatiotemporal variation of SWC into hydrological and atmospheric models (Simmer et al., 2015). Thereby, it is not only important to map SWC at the field and catchment scales but also to gain more insight into the small-scale processes that control flow and transport in the vadose zone and in aquifers.

Geophysical methods have been widely used in the last decades to improve understanding of SWC variability at different scales (Binley et al., 2015). One of the most promising geophysical methods to measure SWC is ground penetrating radar (GPR) because of the high sensitivity of GPR wave velocity to changes in SWC. Furthermore, GPR has the advantage to more directly relate the velocity changes to SWC without the necessity of using empirical relationships (Steelman and Endres, 2011). In addition, the ability of GPR to map SWC at various spatial scales offers a high potential to close the gap between large-scale remote sensing methods and small-scale point measurements. In addition, remote sensing observations are only able to provide information about the upper few centimeters of the vadose zone, but GPR has the potential to provide information about SWC deeper in the soil. In a recent overview of GPR studies focused on groundwater applications, Paz et al. (2017) reviewed 91 case studies and suggested strategies on how GPR can be used to study groundwater-driven ecosystems. The majority of these studies were conducted within the last two decades and highlight the rapid increase in the use of GPR.

In this update, we aim to review advances for measuring SWC with GPR with a focus on the past decade. We consider this update as a companion to Huisman et al. (2003),

which presents the basic theoretical principles of GPR and how they can be used to investigate the spatiotemporal variation of SWC. In particular, four categories of methods to determine SWC with GPR were distinguished in Huisman et al. (2003): (i) single- and multi-offset measurements to determine dielectric permittivity from reflected wave velocity; (ii) dielectric permittivity determination from ground wave velocity; (iii) zero-offset profile and multi-offset borehole GPR measurements to obtain profiles and tomographic images of dielectric permittivity; and (iv) dielectric permittivity determination from the surface reflection coefficient. Since the publication of Huisman et al. (2003), new methods of GPR data acquisition and analysis have been developed, GPR measurement systems have been improved, and the rapid growth of computational power now allows the use of inversion methods that were previously not feasible. Especially, the use of highly sophisticated inversion methods (e.g., Meles et al., 2010), coupled inversions (e.g., Hinnell et al., 2010; Busch et al., 2013), and a change from two- to three-dimensional investigations are now state-of-the-art and applied much more widely (e.g., Truss et al., 2007; Allroggen et al., 2015). Here we critically review recent progress with GPR for vadose zone studies with a focus on advances in multi-offset and borehole GPR measurements, the achievements of quantitative off-ground GPR approaches, the improved resolution that can be achieved with full-waveform inversion, and new insights that can be obtained from time-lapse GPR measurements. Furthermore, the use of GPR data for hydrological parameter estimation is illustrated and recent improvements in GPR instrumentation are discussed.

A Brief Recap of GPR Principles

Ground-penetrating radar considers the propagation of electromagnetic (EM) waves in the subsurface and provides estimates of the relative dielectric permittivity ϵ_r (related to EM wave velocity v) and electrical conductivity σ (related to the attenuation of the EM wave α) of the medium through which the wave travels. The EM waves are emitted by the transmitter antenna (Tx), and the scattered, reflected, and refracted waves are sensed by one or several receiver antennae (Rx). Three different GPR measurement configurations are widely used: surface, borehole, and off-ground measurements. For low-loss and non-magnetic materials, ϵ_r can be obtained from

$$\epsilon_r = \left(\frac{c}{v} \right)^2 \quad [1]$$

where c is the speed of light in free space (0.3 m ns^{-1}). Commercial GPR systems have a center frequency f_c between 50 MHz and 3.6 GHz, and the corresponding wavelength (λ_c) of the signal is $\lambda_c = v/f_c$. Thus, higher frequencies have a smaller wavelength that allows a higher resolution in subsurface characterization to be achieved. At the same time, higher frequencies are more strongly attenuated, which reduces penetration depth. Therefore, there is a fundamental trade-off between resolution and penetration depth in GPR investigations.

Both ϵ_r and σ can be linked to hydrologically relevant parameters, such as SWC, porosity, permeability, lithological variations,

fluid conductivity, and clay and salt content (e.g., Linde et al., 2006; Busch et al., 2014). On the one hand, the large contrast in the relative dielectric permittivity of air ($\epsilon_r = 1$) and water ($\epsilon_r = 80$) can be used to obtain SWC in the vadose zone (e.g., Binley et al., 2002b; Paz et al., 2017) and porosity in the saturated zone (e.g., Dafflon et al., 2011; Klotzsche et al., 2013). On the other hand, the attenuation of EM wave provides information on the electrical conductivity of the medium and can provide indications for clay content (e.g., Looms et al., 2018) or pore water salinity (e.g., Tsoflias and Becker, 2008). To derive SWC or porosity from dielectric permittivity measured with GPR, empirical or more physics-based petrophysical relationships can be used (Steelman and Endres, 2011). The most widely used empirical relationship is Topp's equation (Topp et al., 1980). Alternatively, a wide range of dielectric mixing models is available that relate the bulk permittivity to the volume fraction and permittivity of each of the soil constituents. More detailed information on the basics of GPR can be found in Jol (2009) and Huisman et al. (2003).

Multi-Offset Techniques for Soil Water Content Determination from Reflected Waves

Surface GPR data are commonly acquired in the common-offset reflection profiling mode, with a fixed spacing between the transmitter and the receiver antennae. The obtained radargrams thereby display changes of physical properties in the subsurface across a certain range in positions vs. travel time. This method is easy and fast to apply and can be used for large-scale surveys along lines or on a grid. The travel time of the reflected GPR wave depends on the depth of the reflector and the mean dielectric permittivity (and thus SWC) above the reflector. Therefore, independent information on reflector depth is required to estimate SWC in the case of single-offset measurements (Huisman et al., 2003). Information on the subsurface velocity at certain locations can be obtained using common-midpoint (CMP) or wide-angle reflection and refraction (WARR) measurements, where the transmitter and receiver spacing are varied.

The use of multi-offset data acquisition strategies allows the simultaneous determination of reflector depth and wave velocity and is thus much better suited for SWC estimation. Building on previous work from seismic data processing, Bradford (2008) used reflection tomography and pre-stack depth migration to obtain high-resolution information on vertical and horizontal variations in SWC from multi-offset surface GPR data consisting of 25 different offsets ranging from 1.8 to 16.5 m for each position. However, the acquisition of such multi-offset data is labor intensive because of the need to manually change antenna offsets and thus effectively not suitable for SWC mapping applications.

In the past decade, all major GPR manufacturers have developed systems that allow on-the-fly GPR data acquisition with multiple receiving antennae, although the number of antenna offsets obtained with such multi-channel systems is currently lower than for the quasi-continuous multi-offset data acquisition discussed above. Gerhards et al. (2008) developed a straightforward

interpretation strategy for multichannel GPR data with a limited number of offsets, which allows the high-resolution estimation of reflector depth and SWC with only moderate effort. This strategy has successfully been applied to determine both the SWC and the depth of the active layer of permafrost soils (Wollschläger et al., 2010), as well as the spatiotemporal variation of SWC in a heterogeneous agricultural field (Pan et al., 2012a).

Despite the obvious potential, there are also limitations to the use of multichannel GPR measurements. The most obvious limitation is the need for continuous reflectors that can be unambiguously identified for multiple antenna offsets. In addition, a synthetic modeling study by Pan et al. (2012b) showed that wide offsets (~ 1.5 times the reflector depth) are required to allow accurate determination of reflector depth and SWC, which may be problematic because of increased GPR wave attenuation for larger offsets. Nevertheless, we feel that multichannel GPR measurements are promising for vadose zone hydrology and deserve more attention, also because the ground wave can be better identified and used for SWC mapping using this type of setup.

Waveguide Inversion of Dispersive GPR Data

Whereas it is commonly assumed that the ground wave and reflected wave can be interpreted by assuming a homogeneous SWC distribution, real world scenarios cannot always be simplified to these cases, especially during dynamic hydrological processes such as infiltration and soil thawing, where thin layers with a strong contrast and gradient in permittivity may affect the GPR response. In particular, water infiltration into the soil can result in a high-water-content surface layer, which can act as a low-velocity waveguide and trap the EM waves emitted by the GPR due to the total reflection that occurs beyond the critical angle on the upper and lower interfaces (Arcone et al., 2003). Due to the multiple reflections that interfere, conventional travel-time analysis techniques cannot be reliably applied. Similar to seismic Rayleigh and Love wave analysis, WARR or CMP data can in this case be used to calculate a phase-velocity spectrum, which provides the frequency-dependent phase velocity that can be used in inverse modeling to estimate the medium properties (van der Kruk et al., 2010). Recently, this method has been extended for gradational water content profiles and variable sharpness of a wetting front (Mangel et al., 2015, 2017).

Borehole GPR Vertical Radar Profile Data for Soil Water Content Determination

Traditionally, borehole radar measurements have mainly been made using zero-offset profiles or multi-offset gathers. Recently, the vertical radar profiling (VRP) technique has become more popular. In this data acquisition strategy, the transmitter antenna is placed at the surface at various fixed separations away from the borehole for a range of receiver positions in a single borehole. Several studies have shown the potential of this method to estimate soil hydrological, geological and engineering properties of the critical zone (e.g., Cassiani et al., 2004; Strobach et al., 2014; Tronicke

and Hamann, 2014). The VRP technique provides a good compromise between surface and borehole GPR measurements because it improves the depth of investigation compared with surface GPR measurements and extends the area of investigation to the near surface, where borehole GPR measurements are difficult to interpret because of interference of direct, reflected, and critically refracted waves. In addition, VRP measurements require only a single borehole, which is advantageous because of the limited availability of borehole pairs and the high costs associated with drilling new boreholes. Vertical radar profile data can be used to derive one-dimensional permittivity and attenuation profiles of the subsurface close to the borehole using ray-based approaches by analyzing travel times and amplitudes (Tronicke and Hamann, 2014). However, special care needs to be taken to avoid having direct waves between transmitter and receiver interfere with critically refracted waves, which would violate the assumptions in ray-based inversions of direct travel time and first-cycle amplitude. Therefore, the VRP survey design needs to consider the choice of a range of appropriate separations of the transmitter to the borehole to avoid such interferences.

Off-Ground GPR for Soil Water Content Determination

Off-ground GPR measurements in the time domain have been used for estimating SWC using the surface reflection method (Serbin and Or, 2005). In the past decade, progress has been made in the modeling of off-ground radar signals and, in particular, in accounting for antenna effects. In the antenna-medium model developed by Lambot et al. (2004), a far-field radar antenna is modeled using frequency-dependent global reflection and transmission coefficients, and three-dimensional Green's functions are used to model the frequency response of the soil medium (see example in Fig. 1). In combination with a GPR measurement setup that operates in the frequency domain and consists of a vector network analyzer connected to a monostatic ultra-wideband horn antenna (see Fig. 1a), inverse modeling with the antenna-medium model is used to estimate SWC. The method proved to be particularly appropriate for field-scale SWC monitoring and mapping at a high spatial resolution as well as for validating air- and spaceborne radar data due to its rapidity and mobility of the air-launched configuration as shown in Fig. 1 (Jonard et al., 2013; Minet et al., 2012). Recently, Lambot and André (2014) generalized the original far-field antenna-medium model to near-field conditions using an equivalent set of source and field points.

Compared with on-ground GPR systems, the off-ground configuration is less suited to obtain information from deep soil horizons due to the strong dielectric contrast at the soil-air interface that reflects a considerable part of the energy and thus reduces the reflection strength from subsurface layers. Another drawback of the off-ground GPR method is the sensitivity to soil surface roughness. Recent work has shown that surface roughness can be accounted for in the inversion of off-ground GPR data for SWC retrieval by combining a roughness model with the

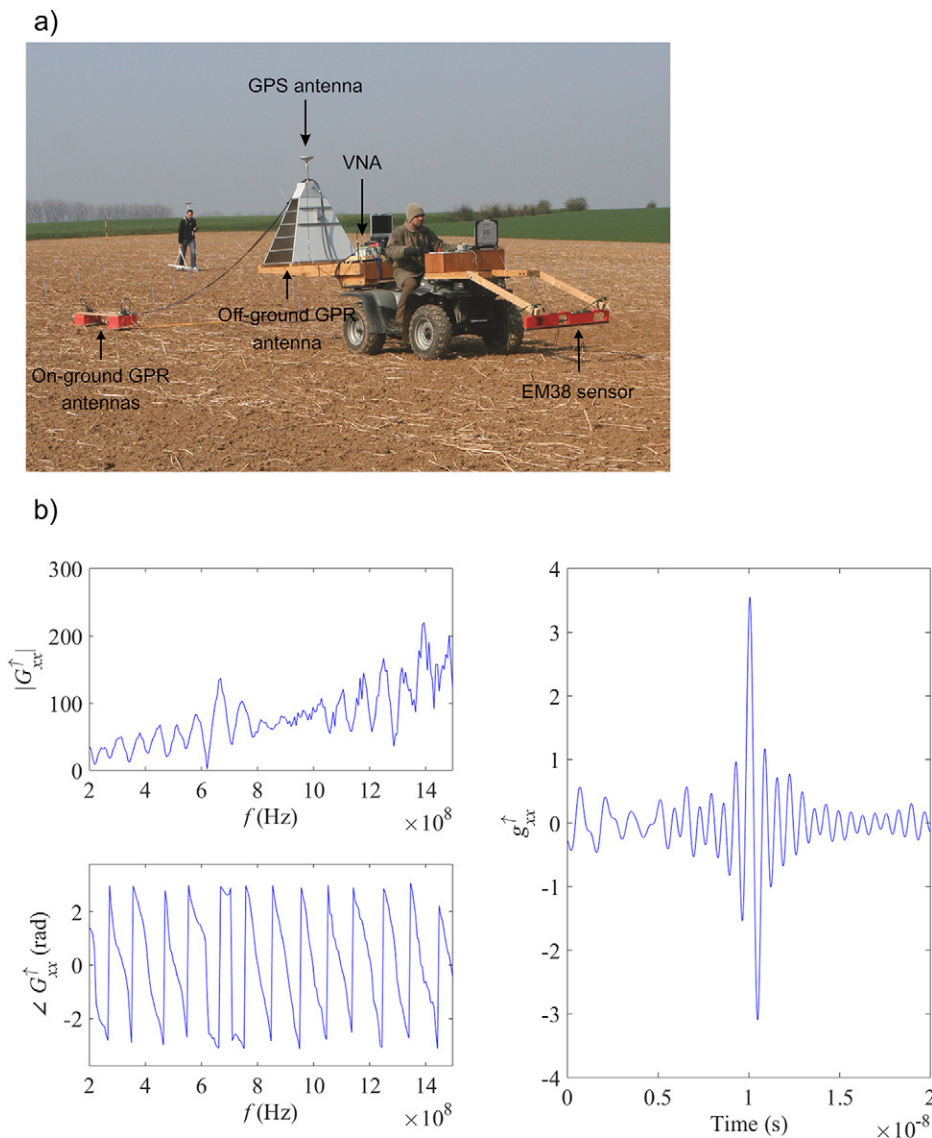


Fig. 1. (a) An off-ground GPR system (vector network analyzer [VNA] connected to a horn antenna, differential GPS device, and a PC) as well as an on-ground GPR and an EM38 sensor mounted on a quad (adapted from Jonard et al., 2013); (b) GPR Green's function in the frequency and time domains ($|G_{xx}^f|$ and $\angle G_{xx}^f$ denote the amplitude and the phase, respectively, of the Green's function in the frequency domain and g_{xx}^t represents the Green's function in the time domain) computed from the raw GPR data S_{11} measured by the VNA at the location shown. A clear soil surface reflection can be observed around 10 ns on the plot of the Green's function in the time domain.

antenna-medium model (Jonard et al., 2012). Nevertheless, large and oriented soil surface roughness cannot be properly accounted for and may lead to inaccurate SWC estimations.

Full-Waveform Inversion of GPR Data

Ongoing improvements in computer power and the widespread availability of high-performance cluster computers allow the application of more computationally demanding approaches for GPR data analysis, such as full-waveform inversion (FWI). Full-waveform inversion has been successfully used in seismic exploration since the 1980s, and it is widely considered to be a promising tool to improve the resolution of subsurface characterization. In the past decade, FWI has been adapted for GPR (e.g., Meles et al., 2010). Compared with standard ray-based inversion schemes that use a small amount of the measured data (e.g., first arrival time and first cycle amplitude), FWI allows characterization of the subsurface with a higher resolution in terms of ϵ_r and σ . Since the introduction of FWI for GPR data, it has been continuously improved, and multiple field applications using multi-offset

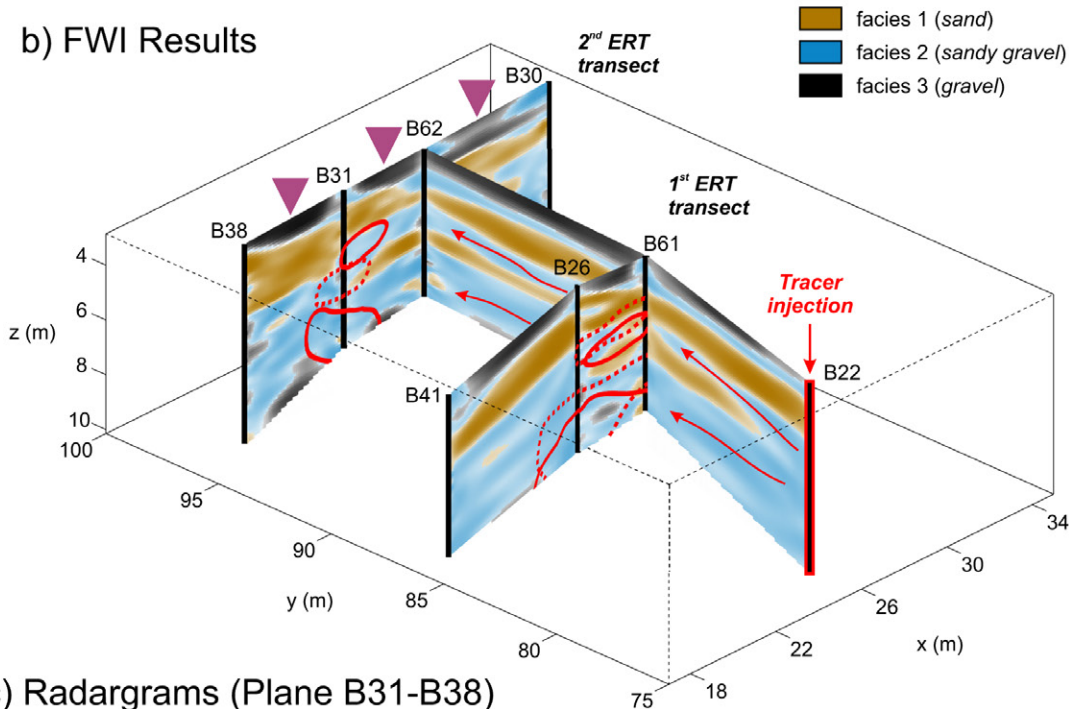
crosshole GPR data have been developed where decimeter-scale subsurface features have been resolved, including the characterization of aquifers (Klotzsche et al., 2013; Gueting et al., 2017), karst (Keskinen et al., 2017), and clayey till (Looms et al., 2018).

Several case studies have shown that aquifer porosity estimates obtained from FWI of GPR data were in good agreement with independently measured logging data (e.g., Klotzsche et al., 2014). In addition, Klotzsche et al. (2013) showed that FWI was able to identify a high-permittivity and -porosity layer that correlated to zones of preferential flow with a higher saturated hydraulic conductivity within the aquifer. This feature was not retrieved by standard ray-based inversion due to the lower resolution, demonstrating that FWI can resolve connected small-scale structures that can have an important contribution to flow and transport in aquifers. The first large-scale application of FWI was performed by Gueting et al. (2017) at the Krauthausen site in Germany (Fig. 2a), where several crosshole planes were stitched together to a 25- by 50-m domain with an investigation depth of up to 11 m (Fig. 2b). Generally, a good fit between the FWI modeled data and the measured data was

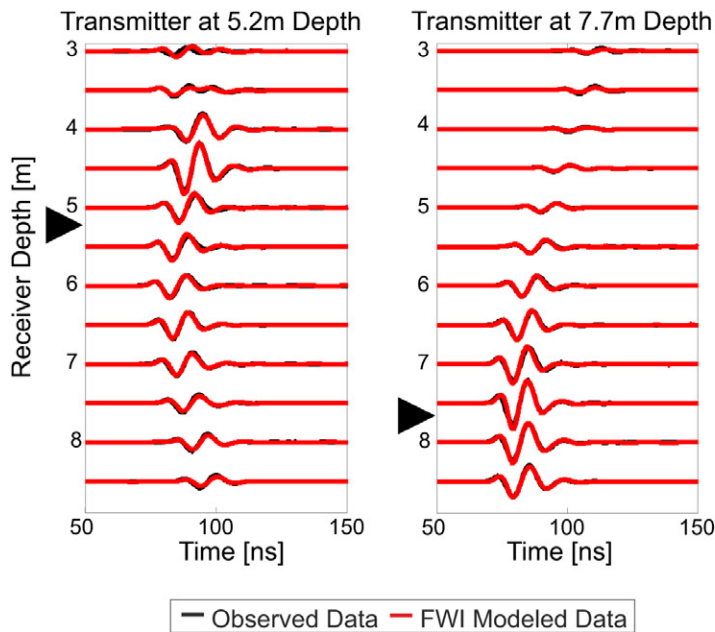
a) Borehole GPR Measurements



b) FWI Results



c) Radargrams (Plane B31-B38)



d) Porosity Comparison

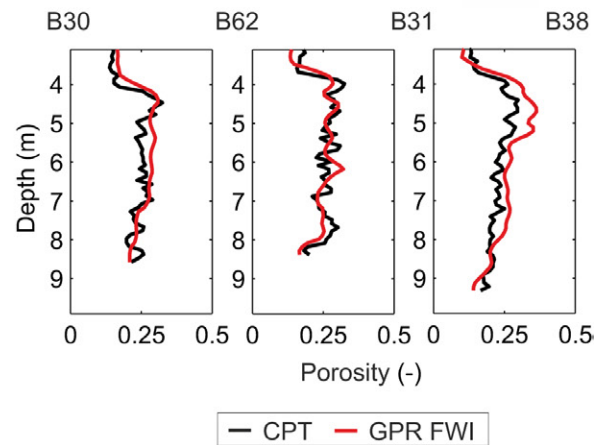


Fig. 2. (a) Setup of GPR borehole measurements at the Krauthausen test site; (b) GPR full-waveform inversion (FWI) cluster analysis results of the site, showing a tracer plume splitting in the aquifer due to a less permeable layer that was previously deduced from time-lapse electrical resistivity tomography (ERT) measurements; (c) example observed and FWI modeled radargrams of Plane 31 to 38 in black and red, respectively, with a black arrow indicating the position of the transmitter; and (d) comparison of porosity derived from cone penetration test (CPT) data (black) and FWI permittivity estimates (red). The locations are indicated in (b) with violet arrows. Data based on Gueting et al. (2017).

obtained for all the investigated data (an example is provided in Fig. 2c). Different lithological facies were identified by applying a cluster analysis and a comparison with porosity (see Fig. 2b and 2d), and hydraulic conductivity measurements from direct-push, flowmeter and grain size data indicated that the facies distribution obtained with FWI was hydrogeologically meaningful. In particular, the derived facies distribution was able to explain a tracer plume splitting in the aquifer due to a less permeable layer that was previously deduced from time-lapse electrical resistivity tomography (ERT) measurements (Fig. 2b; Müller et al., 2010).

Full-waveform inversion has also been applied to off-ground and surface GPR measurements. In fact, the off-ground GPR approach of Lambot et al. (2004) described above can also be considered as a FWI approach. For both types of data, the subsurface is typically assumed to be a horizontally layered medium. In the inversion, profiles of permittivity and electrical conductivity are estimated from the ground wave (Busch et al., 2014) or off-ground reflection data (Lambot et al., 2009).

The Value of Time-Lapse Observations

Ground-penetrating radar measurements are ideally suited for time-lapse investigations due to the nondestructive nature of the method. Interestingly, changes in radar velocity, and thereby changes in SWC, are independent of the lithological parameters used in a dielectric mixing model, making them more reliable than absolute SWC estimates (Binley et al., 2002b). As a result, the accuracy and repeatability of time-lapse borehole GPR measurements can be very high. Binley et al. (2002b) showed the ability of time-lapse GPR measurements to follow infiltration fronts associated with natural infiltration down to a depth of 15 m. At this depth, small seasonal SWC changes of 0.005 to $0.01 \text{ cm}^3 \text{ cm}^{-3}$ could be detected. Other studies have also used GPR to investigate downward water flow in thick vadose zones (Deiana et al., 2008). The result of such a study is shown in Fig. 3. Here, subsurface SWC changes are observed in unsaturated sand sediments following temporal changes in net precipitation (= precipitation – potential evapotranspiration). Most studies have indicated small SWC variations of up to $0.03 \text{ cm}^3 \text{ cm}^{-3}$ associated with natural infiltration. However, this may be a biased view because GPR studies have predominantly been conducted in materials with a low electrical conductivity that typically also have a low water retention capability. In addition, measurements from the upper 1.0 to 1.5 m of the subsurface, including the dynamic root zone, are often not analyzed because borehole GPR measurements are difficult to interpret near the surface due to the interference of direct and critically refracted waves.

To create time-lapse borehole GPR observations with a larger hydrological response, forced infiltration experiments with point sources (Binley et al., 2002a; Haarder et al., 2012), trenches (Deiana et al., 2008), or areal infiltration experiments (Looms et al., 2008), as well as gas injection experiments (Lassen et al., 2015; Steelman et al., 2017) have been conducted. This ensures that time-lapse observations contain more information regarding the

subsurface flow properties. A major challenge in this type of study is that geological variability may cause the injected water or gas to migrate laterally out of the subsurface volume that can be investigated by borehole GPR measurements. For example, Haarder et al. (2012) observed lateral water diversion after only a few meters of vertical flow from the injection point, which was attributed to thin non-horizontal layers of sand with different silt fractions.

Alternatively, time-lapse surface GPR measurements can be used to investigate the near-surface environment (e.g., Mangel et al., 2017; Pan et al., 2012b). Trinks et al. (2001) monitored a point injection experiment into an unsaturated sandbox and used difference plots to visualize the affected infiltration area. Truss et al. (2007) monitored both natural and forced infiltration into an oolitic limestone and quantified the travel time delay of selected reflectors. Klenk et al. (2015) studied soil water dynamics at an artificially controlled test site and estimated SWC changes from reflection data. In addition, they analyzed the detectability of the capillary fringe from GPR reflections. In all these studies, a critical issue was to meticulously repeat the measurements along the exact same reflection profile because local changes near the emitting antenna can substantially alter the signal. Additionally, the absolute SWC value or change in SWC can only be obtained in the case where information regarding the depths to the reflectors is known (Huisman et al., 2003).

Hydrological Model Parameterization Using GPR Data

The availability of time-lapse GPR measurements of water content naturally leads to the question whether hydrological models for unsaturated flow can be parameterized using this type of measurement. Binley et al. (2002a) used a relatively simple parameterization strategy where the moments of the measured SWC distribution were used to estimate soil hydraulic properties. More advanced approaches where the GPR travel time data are used directly to estimate hydraulic parameters without using a geophysical inversion first (often named *coupled inversion* or *integrated data fusion*) have also been proposed for borehole (Kowalsky et al., 2004; Looms et al., 2008), surface (Busch et al., 2013), and off-ground GPR data (Lambot et al., 2009). This is done to avoid having geophysical inversion artifacts arising from regularization propagate to the estimated hydraulic parameters and to provide additional constraints to the typically ill-posed inverse problem of estimating hydraulic parameters from SWC data. Nevertheless, it is important to realize that hydraulic parameters estimated from GPR data (and any other SWC sensor) can be quite uncertain. Therefore, many studies also determined model parameter uncertainty with informal (Binley and Beven, 2003; Looms et al., 2008) or formal Bayesian approaches (Kowalsky et al., 2004; Jonard et al., 2015). The results of these studies typically showed that GPR data mostly contained sufficient information to constrain the saturated hydraulic conductivity but that there was less information to constrain parameters of the water retention function (Binley and Beven, 2003; Scholer et al., 2012). One possible strategy to add information to this highly underdetermined inversion problem is to consider multiple measurement

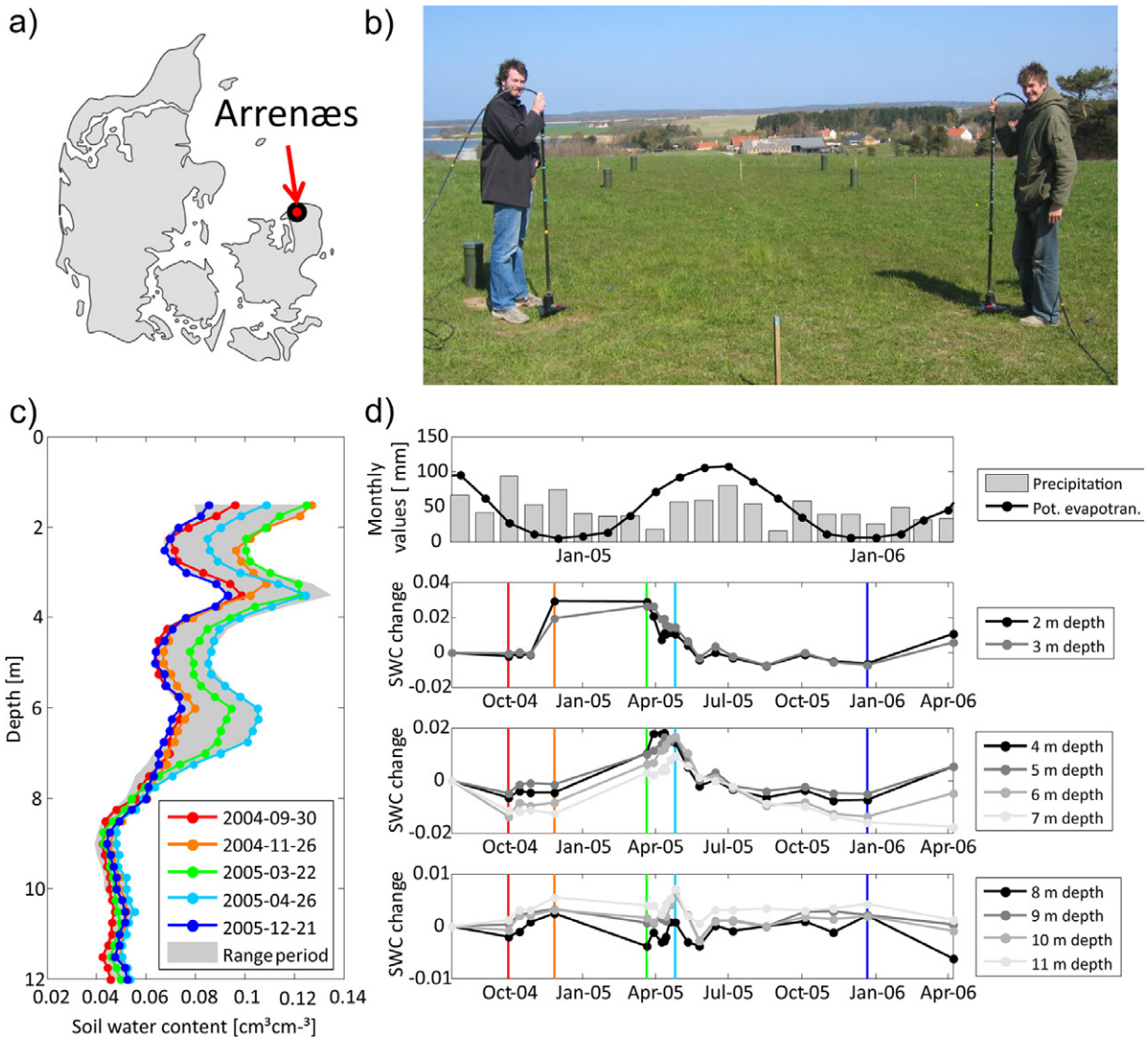


Fig. 3. Seasonal soil water content change measured in sandy sediments by crosshole GPR at the Arrenæs field site in Denmark, where a total of 21 measurement surveys (zero-offset profiles [ZOPs]) were collected between 21 July 2004 and 7 Apr. 2006 showing the vertical water flux arising from periods with surplus net precipitation (= precipitation – potential evapotranspiration): (a) the field site location; (b) the field site during a calibration measurement using 100 MHz antennae; (c) five selected ZOP profiles showing the estimated average soil water content as a function of depth, and the entire soil water content range recorded during all 21 ZOPs illustrated in grey; and (d) soil water content (SWC) time series at selected depths estimated from the 21 measurement surveys, along with precipitation and potential evapotranspiration time series for the field site location.

types. For this reason, many studies have considered additional measurements in the inversion, such as hydrological measurements (Kowalsky et al., 2004), and other geophysical measurements such as ERT (e.g., Looms et al., 2008). Additionally, accurate knowledge of the hydrologically relevant subsurface structures (e.g., layering) affecting flow and transport processes can be obtained directly by GPR measurements (Steelman et al., 2012; Gueting et al., 2017). The inclusion of such structural information about subsurface architecture into hydrological models obviously also is highly relevant and will improve hydrological model predictions.

Development of GPR Instrumentation

Ground-penetrating radar systems have benefited from faster and more stable electronic components that continuously become

available on the market. This has resulted in a higher measurement quality and increased data acquisition speed, which, for example, allows faster acquisition of multichannel GPR measurements. Accurate positioning of GPR measurements is important, and most GPR systems now allow a plug-and-play connection with GPS systems to determine accurate positions for each measured GPR trace. Using a single-frequency GPS system, the positional accuracy may not be sufficient for every application. Differential GPS approaches need to be used when a high positional accuracy is required. In this case, absolute and relative geographical coordinates of the GPS rover can be determined with an accuracy of about 0.20 to 0.40 and 0.02 to 0.05 m, respectively. However, the drawback of such GPS systems is the need for post-processing of the GPS data. Another option is to use mobile phone communication from a base station

to avoid post-processing. Recently, a new GPS approach has become commercially available that receives the differential signal via satellite communication (the European Geostationary Navigation Overlay Service [EGNOS] and Wide Area Augmentation System [WAAS]) instead of a base station. In this way, no post-processing is necessary anymore, and an absolute positional accuracy up to 0.04 m can be achieved. In areas without good GPS signal coverage, a high positional accuracy can only be achieved with a self-tracking total station (Böniger and Tronicke, 2010).

Conclusions and the Road Ahead

In this update, we have highlighted recent developments and achievements for measuring and monitoring SWC with GPR. In particular, improved and faster data acquisition approaches, such as continuous multi-offset measurements, off-ground GPR measurements, three-dimensional measurements, and VRP have been presented. The rapid increase in computational power has also enabled sophisticated inversion methods for GPR, including FWI to obtain subsurface information with higher spatial resolution and coupled inversion to obtain hydraulic parameters from time-lapse GPR measurements. Many advances presented here rely on advanced GPR data processing. These processing procedures have not reached a level of maturity such that they can be readily applied by non-experts. In our opinion, it should be a goal of the next generation of developments to enable the use of these techniques by non-experts. Finally, it is expected that ongoing instrumental developments will allow high-speed multichannel GPR measurements to map SWC at the field and perhaps even the catchment scale. Despite the high potential of GPR for hydrological investigations, it is important to realize that no single geophysical method will perform optimally under all conditions. For example, GPR is mostly restricted to areas with relatively low electrical conductivity (low attenuation of the EM wave). In addition, some of the GPR interpretation methods require the presence of well identifiable and continuous GPR reflections, which requires sufficient and spatially continuous subsurface contrast in dielectric permittivity. If these conditions are not satisfied, other geophysical methods may be more suitable.

Acknowledgments

We acknowledge the support by the SFB/TR32 "Pattern in Soil–Vegetation–Atmosphere Systems: Monitoring, Modelling, and Data Assimilation" funded by the Deutsche Forschungsgemeinschaft (DFG). We thank Markus Flury (associate editor), Ute Wollschläger (reviewer), and an anonymous reviewer for their constructive review. A. Klotzsche is supported by the Helmholtz Postdoc Programme.

References

- Allroggen, N., L.M.B. van Schaik, and J. Tronicke. 2015. 4D ground-penetrating radar during a plot scale dye tracer experiment. *J. Appl. Geophys.* 118:139–144. doi:10.1016/j.jappgeo.2015.04.016
- Arcone, S.A., P.R. Peapples, and L.B. Liu. 2003. Propagation of a ground-penetrating radar (GPR) pulse in a thin-surface waveguide. *Geophysics* 68:1922–1933. doi:10.1190/1.1635046
- Binley, A., and K. Beven. 2003. Vadose zone flow model uncertainty as conditioned on geophysical data. *Ground Water* 41:119–127. doi:10.1111/j.1745-6584.2003.tb02576.x
- Binley, A., G. Cassiani, R. Middleton, and P. Winship. 2002a. Vadose zone flow model parameterisation using cross-borehole radar and resistivity imaging. *J. Hydrol.* 267:147–159. doi:10.1016/S0022-1694(02)00146-4
- Binley, A., S.S. Hubbard, J.A. Huisman, A. Revil, D.A. Robinson, K. Singha, and L.D. Slater. 2015. The emergence of hydrogeophysics for improved understanding of subsurface processes over multiple scales. *Water Resour. Res.* 51:3837–3866.
- Binley, A., P. Winship, L.J. West, M. Pokar, and R. Middleton. 2002b. Seasonal variation of moisture content in unsaturated sandstone inferred from borehole radar and resistivity profiles. *J. Hydrol.* 267:160–172. doi:10.1016/S0022-1694(02)00147-6
- Böniger, U., and J. Tronicke. 2010. On the potential of kinematic GPR surveying using a self-tracking total station: Evaluating system crosstalk and latency. *IEEE Trans. Geosci. Remote Sens.* 48:3792–3798. doi:10.1109/TGRS.2010.2048332
- Bradford, J.H. 2008. Measuring water content heterogeneity using multifold GPR with reflection tomography. *Vadose Zone J.* 7:184–193. doi:10.2136/vzj2006.0160
- Busch, S., J. van der Kruk, and H. Vereecken. 2014. Improved characterization of fine-texture soils using on-ground GPR full-waveform inversion. *IEEE Trans. Geosci. Remote Sens.* 52:3947–3958. doi:10.1109/TGRS.2013.2278297
- Busch, S., L. Weihermüller, J.A. Huisman, C.M. Steelman, A.L. Endres, H. Vereecken, and J. van der Kruk. 2013. Coupled hydrogeophysical inversion of time-lapse surface GPR data to estimate hydraulic properties of a layered subsurface. *Water Resour. Res.* 49:8480–8494. doi:10.1002/2013WR013992
- Cassiani, G., C. Strobbia, and L. Gallotti. 2004. Vertical radar profiles for the characterization of deep vadose zones. *Vadose Zone J.* 3:1093–1105. doi:10.2136/vzj2004.1093
- Dafflon, B., J. Irving, and W. Barrash. 2011. Inversion of multiple intersecting high-resolution crosshole GPR profiles for hydrological characterization at the Boise Hydrogeophysical Research Site. *J. Appl. Geophys.* 73:305–314. doi:10.1016/j.jappgeo.2011.02.001
- Deiana, R., G. Cassiani, A. Villa, A. Bagliani, and V. Bruno. 2008. Calibration of a vadose zone model using water injection monitored by GPR and electrical resistance tomography. *Vadose Zone J.* 7:215–226. doi:10.2136/vzj2006.0137
- Famiglietti, J.S., D.R. Ryu, A.A. Berg, M. Rodell, and T.J. Jackson. 2008. Field observations of soil moisture variability across scales. *Water Resour. Res.* 44:W01423. doi:10.1029/2006WR005804
- Gerhards, H., U. Wollschläger, Q.H. Yu, P. Schiwek, X.C. Pan, and K. Roth. 2008. Continuous and simultaneous measurement of reflector depth and average soil-water content with multichannel ground-penetrating radar. *Geophysics* 73:J15–J23. doi:10.1190/1.2943669
- Gueing, N., T. Vienken, A. Klotzsche, J. van der Kruk, J. Vanderborght, J. Caers, et al. 2017. High resolution aquifer characterization using crosshole GPR full-waveform tomography: Comparison with direct-push and tracer test data. *Water Resour. Res.* 53:49–72. doi:10.1002/2016WR019498
- Haarder, E.B., A. Binley, M.C. Looms, J. Doetsch, L. Nielsen, and K.H. Jensen. 2012. Comparing plume characteristics inferred from cross-borehole geophysical data. *Vadose Zone J.* 11(4). doi:10.2136/vzj2012.0031
- Hinnell, A.C., T.P.A. Ferré, J.A. Vrugt, J.A. Huisman, S. Moysey, J. Rings, and M.B. Kowalsky. 2010. Improved extraction of hydrologic information from geophysical data through coupled hydrogeophysical inversion. *Water Resour. Res.* 46:W00D40. doi:10.1029/2008WR007060
- Huisman, J.A., S.S. Hubbard, J.D. Redman, and P.A. Annan. 2003. Measuring soil water content with ground penetrating radar: A review. *Vadose Zone J.* 2:476–491. doi:10.2136/vzj2003.4760
- Jol, H.M., editor. 2009. *Ground penetrating radar: Theory and applications*. Elsevier Science, Amsterdam.
- Jonard, F., M. Mahmoudzadeh, C. Roisin, L. Weihermüller, F. André, J. Minet, et al. 2013. Characterization of tillage effects on the spatial variation of soil properties using ground-penetrating radar and electromagnetic induction. *Geoderma* 207–208:310–322. doi:10.1016/j.geoderma.2013.05.024
- Jonard, F., L. Weihermüller, M. Schwank, K.Z. Jadoon, H. Vereecken, and S. Lambot. 2015. Estimation of hydraulic properties of a sandy soil using ground-based active and passive microwave remote sensing. *IEEE Trans. Geosci. Remote Sens.* 53:3095–3109. doi:10.1109/TGRS.2014.2368831

- Jonard, F., L. Weihermüller, H. Vereecken, and S. Lambot. 2012. Accounting for soil surface roughness in the inversion of ultrawideband off-ground GPR signal for soil moisture retrieval. *Geophysics* 77:H1–H7. doi:10.1190/geo2011-0054.1
- Keskinen, J., A. Klotzsche, M.C. Looms, J. Moreau, J. van der Kruk, K. Holliger, et al. 2017. Full-waveform inversion of crosshole GPR data: Implications for porosity estimation in chalk. *J. Appl. Geophys.* 140:102–116. doi:10.1016/j.jappgeo.2017.01.001
- Klenk, P., S. Jaumann, and K. Roth. 2015. Quantitative high-resolution observations of soil water dynamics in a complicated architecture using time-lapse ground-penetrating radar. *Hydrol. Earth Syst. Sci.* 19:1125–1139. doi:10.5194/hess-19-1125-2015
- Klotzsche, A., J. van der Kruk, J. Bradford, and H. Vereecken. 2014. Detection and identification of waveguides with limited lateral extent using an amplitude analysis approach and crosshole GPR full-waveform inversion: Synthetic and experimental data. *Water Resour. Res.* 50:6966–6985. doi:10.1002/2013WR015177
- Klotzsche, A., J. van der Kruk, N. Linde, J. Doetsch, and H. Vereecken. 2013. 3-D characterization of high-permeability zones in a gravel aquifer using 2-D crosshole GPR full-waveform inversion and waveguide detection. *Geophys. J. Int.* 195:932–944. doi:10.1093/gji/ggt275
- Kowalsky, M.B., S. Finsterle, and Y. Rubin. 2004. Estimating flow parameter distributions using ground-penetrating radar and hydrological measurements during transient flow in the vadose zone. *Adv. Water Resour.* 27:583–599. doi:10.1016/j.advwatres.2004.03.003
- Lambot, S., and F. André. 2014. Full-wave modeling of near-field radar data for planar layered media reconstruction. *IEEE Trans. Geosci. Remote Sens.* 52:2295–2303. doi:10.1109/TGRS.2013.2259243
- Lambot, S., E. Slob, J. Rhebergen, O. Lopera, K.Z. Jadoon, and H. Vereecken. 2009. Remote estimation of the hydraulic properties of a sand using full-waveform integrated hydrogeophysical inversion of time-lapse, off-ground GPR data. *Vadose Zone J.* 8:743–754. doi:10.2136/vzj2008.0058
- Lambot, S., E.C. Slob, I. van den Bosch, B. Stockbroeckx, and M. Vanclooster. 2004. Modeling of ground-penetrating radar for accurate characterization of subsurface electric properties. *IEEE Trans. Geosci. Remote Sens.* 42:2555–2568. doi:10.1109/TGRS.2004.834800
- Lassen, R.N., T.O. Sonnenborg, K.H. Jensen, and M.C. Looms. 2015. Monitoring CO₂ gas-phase migration in a shallow sand aquifer using cross-borehole ground penetrating radar. *Int. J. Greenhouse Gas Control* 37:287–298. doi:10.1016/j.ijggc.2015.03.030
- Linde, N., A. Binley, A. Tryggvason, L.B. Pedersen, and A. Revil. 2006. Improved hydro-geophysical characterization using joint inversion of cross-hole electrical resistance and ground-penetrating radar travel-time data. *Water Resour. Res.* 42:W12404. doi:10.1029/2006WR005131
- Looms, M.C., A. Binley, K.H. Jensen, L. Nielsen, and T.M. Hansen. 2008. Identifying unsaturated hydraulic parameters using an integrated data fusion approach on cross-borehole geophysical data. *Vadose Zone J.* 7:238–248. doi:10.2136/vzj2007.0087
- Looms, M.C., A. Klotzsche, J. van der Kruk, T. Hauerberg Larsen, A. Edsen, N. Tuxen, et al. 2018. Mapping sand layers in clayey till using crosshole ground-penetrating radar. *Geophysics* 83:A21–A26. doi:10.1190/geo2017-0297.1
- Mangel, A., S.M. Moysey, and J. van der Kruk. 2015. Resolving precipitation induced water content profiles by inversion of dispersive GPR data: A numerical study. *J. Hydrol.* 525:496–505. doi:10.1016/j.jhydrol.2015.04.011
- Mangel, A., S.M.J. Moysey, and J. van der Kruk. 2017. Resolving infiltration-induced water content profiles by inversion of dispersive ground-penetrating radar data. *Vadose Zone J.* 16(10). doi:10.2136/vzj2017.02.0037
- Meles, G.A., J. van der Kruk, S.A. Greenhalgh, J.R. Ernst, H. Maurer, and A.G. Green. 2010. A new vector waveform inversion algorithm for simultaneous updating of conductivity and permittivity parameters from combination crosshole/borehole-to-surface GPR data. *IEEE Trans. Geosci. Remote Sens.* 48:3391–3407. doi:10.1109/TGRS.2010.2046670
- Minet, J., P. Bogaert, M. Vanclooster, and S. Lambot. 2012. Validation of ground penetrating radar full-waveform inversion for field scale soil moisture mapping. *J. Hydrol.* 424–425:112–123. doi:10.1016/j.jhydrol.2011.12.034
- Müller, K., J. Vanderborght, A. Englert, A. Kemna, J.A. Huisman, J. Rings, and H. Vereecken. 2010. Imaging and characterization of solute transport during two tracer tests in a shallow aquifer using electrical resistivity tomography and multilevel groundwater samplers. *Water Resour. Res.* 46:W03502. doi:10.1029/2008WR007595
- Pan, X., U. Wollschläger, H. Gerhards, and K. Roth. 2012b. Optimization of multi-channel ground-penetrating radar for quantifying field-scale soil water dynamics. *J. Appl. Geophys.* 82:101–109. doi:10.1016/j.jappgeo.2012.02.007
- Pan, X., J. Zhang, P. Huang, and K. Roth. 2012a. Estimating field-scale soil water dynamics at a heterogeneous site using multi-channel GPR. *Hydrol. Earth Syst. Sci.* 16:4361–4372. doi:10.5194/hess-16-4361-2012
- Paz, C., F.J. Alcalá, J.M. Carvalho, and L. Ribeiro. 2017. Current uses of ground penetrating radar in groundwater-dependent ecosystems research. *Sci. Total Environ.* 595:868–885. doi:10.1016/j.scitotenv.2017.03.210
- Scholer, M., J. Irving, M.C. Looms, L. Nielsen, and K. Holliger. 2012. Bayesian Markov-chain-Monte-Carlo inversion of time-lapse crosshole GPR data to characterize the vadose zone at the Arrenaes site, Denmark. *Vadose Zone J.* 11(4). doi:10.2136/vzj2011.0153
- Serbin, G., and D. Or. 2005. Ground-penetrating radar measurement of crop and surface water content dynamics. *Remote Sens. Environ.* 96:119–134. doi:10.1016/j.rse.2005.01.018
- Simmer, C., I. Thiele-Eich, M. Masbou, W. Amelung, H. Bogen, S. Crewell, et al. 2015. Monitoring and modeling the terrestrial system from pores to catchments. *Bull. Am. Meteorol. Soc.* 96:1765–1787. doi:10.1175/BAMS-D-13-00134.1
- Steelman, C.M., and A.L. Endres. 2011. Comparison of petrophysical relationships for soil moisture estimation using GPR ground waves. *Vadose Zone J.* 10:270–285. doi:10.2136/vzj2010.0040
- Steelman, C.M., A.L. Endres, and J.P. Jones. 2012. High-resolution ground-penetrating radar monitoring of soil moisture dynamics: Field results, interpretation, and comparison with unsaturated flow model. *Water Resour. Res.* 48:W09538. doi:10.1029/2011WR011414
- Steelman, C.M., D.R. Klazinga, A.G. Cahill, A.L. Endres, and B.L. Parker. 2017. Monitoring the evolution and migration of a methane gas plume in an unconfined sandy aquifer using time-lapse GPR and ERT. *J. Contam. Hydrol.* 205:12–24. doi:10.1016/j.jconhyd.2017.08.011
- Strobach, E., B.D. Harris, J.C. Dupuis, and A.W. Kepic. 2014. Time-lapse borehole radar for monitoring rainfall infiltration through podsol horizons in a sandy vadose zone. *Water Resour. Res.* 50:2140–2163. doi:10.1002/2013WR014331
- Topp, G.C., J.L. Davis, and A.P. Annan. 1980. Electromagnetic determination of soil water content: Measurements in coaxial transmission lines. *Water Resour. Res.* 16:574–582. doi:10.1029/WR016i003p00574
- Trinks, I., D. Wachsmuth, and H. Stümpel. 2001. Monitoring water flow in the unsaturated zone using georadar. *First Break* 19:679–684. doi:10.1046/j.1365-2397.2001.00228.x
- Tronicke, J., and G. Hamann. 2014. Vertical radar profiling: Combined analysis of traveltimes, amplitudes, and reflections. *Geophysics* 79:H23–H35. doi:10.1190/geo2013-0428.1
- Truss, S., M. Grasmueck, S. Vega, and D.A. Viggiano. 2007. Imaging rainfall drainage within the Miami oolitic limestone using high-resolution time-lapse ground-penetrating radar. *Water Resour. Res.* 43:W03405. doi:10.1029/2005WR004395
- Tsofilas, G.P., and M.W. Becker. 2008. Ground-penetrating-radar response to fracture-fluid salinity: Why lower frequencies are favorable for resolving salinity changes. *Geophysics* 73:J25–J30. doi:10.1190/1.2957893
- van der Kruk, J., R.W. Jacob, and H. Vereecken. 2010. Properties of precipitation induced multi-layer surface waveguides derived from inversion of dispersive TE and TM GPR Data. *Geophysics* 75:WA263–WA273. doi:10.1190/1.3467444
- Vereecken, H., A. Schnepf, J.W. Hopmans, M. Javaux, D. Or, T. Roose, et al. 2016. Modeling soil processes: Review, key challenges, and new perspectives. *Vadose Zone J.* 15(5). doi:10.2136/vzj2015.09.0131
- Wollschläger, U., H. Gerhards, Q. Yu, and K. Roth. 2010. Multi-channel ground-penetrating radar to explore spatial variations in thaw depth and moisture content in the active layer of a permafrost site. *Cryosphere* 4:269–283. doi:10.5194/tc-4-269-2010